Genetically Targeted T Cells Eradicate Systemic Acute Lymphoblastic Leukemia Xenografts

Renier J. Brentjens,[1] Elmer Santos,[2] Yan Nikhamin,[1] Raymond Yeh,[1] Maiko Matsushita,[1] Krista La Perle,[3] Alfonso Quintás-Cardama,[1] Steven M. Larson,[2] and Michel Sadelain[1,4,5]

Abstract

Purpose: Human T cells targeted to the B cell – specific CD19 antigen through retroviral-mediated transfer of a chimeric antigen receptor (CAR), termed 19z1, have shown significant but partial *in vivo* antitumor efficacy in a severe combined immunodeficient (SCID)-Beige systemic human acute lymphoblastic leukemia (NALM-6) tumor model. Here, we investigate the etiologies of treatment failure in this model and design approaches to enhance the efficacy of this adoptive strategy.

Experimental Design: A panel of modified CD19-targeted CARs designed to deliver combined activating and costimulatory signals to the T cell was generated and tested *in vitro* to identify an optimal second-generation CAR. Antitumor efficacy of T cells expressing this optimal costimulatory CAR, 19-28z, was analyzed in mice bearing systemic costimulatory ligand-deficient NALM-6 tumors.

Results: Expression of the 19-28z CAR, containing the signaling domain of the CD28 receptor, enhanced systemic T-cell antitumor activity when compared with 19z1 in treated mice. A treatment schedule of 4 weekly T-cell injections, designed to prolong *in vivo* T-cell function, further improved long-term survival. Bioluminescent imaging of tumor in treated mice failed to identify a conserved site of tumor relapse, consistent with successful homing by tumor-specific T cells to systemic sites of tumor involvement.

Conclusions: Both *in vivo* costimulation and repeated administration enhance eradication of systemic tumor by genetically targeted T cells. The finding that modifications in CAR design as well as T-cell dosing allowed for the complete eradication of systemic disease affects the design of clinical trials using this treatment strategy.

The majority of adult B-cell malignancies, including acute lymphoblastic leukemia (ALL), chronic lymphocytic leukemia, and non – Hodgkin's lymphoma, are incurable despite currently available therapies. For this reason, novel therapeutic strategies are needed to treat these diseases. Adoptive therapy with genetically engineered autologous T cells is one such approach. T cells may be modified to target tumor-associated antigens through the introduction of genes encoding artificial T-cell receptors, termed chimeric antigen receptors (CAR), specific to such antigens (1 – 5).

CD19 is an attractive target for immune-mediated therapies as it is expressed on most B-cell malignancies and normal B cells, but not on bone marrow stem cells. We previously constructed a "first-generation" CAR, termed 19z1, specific to the CD19 antigen. The 19z1 CAR contains a CD19-specific murine single-chain fragment length antibody (scFv) fused to the extracellular and transmembrane regions of CD8, which, in turn, is fused to the intracellular signaling domain of the CD3 ζ chain. Human T cells retrovirally transduced to express the 19z1 receptor specifically lyse heterologous and autologous $CD19^+$ human tumor cells *in vitro* (6). A single i.v. injection of $19z1^+$ T cells into SCID-Beige mice bearing established systemic Raji tumor, a human Burkitt lymphoma tumor cell line that expresses the costimulatory ligands CD80 and CD86, successfully eradicates disease in 50% of mice (6). Unfortunately, a similar therapy fails to fully eradicate systemic NALM-6 tumor, a human pre-B cell ALL cell line that lacks expression of both CD80 and CD86. However, $19z1^+$ T-cell therapy of SCID-Beige mice bearing systemic NALM-6 tumors genetically engineered to express CD80 (NALM-6/CD80) enhanced long-term survival and resulted in complete NALM-6/CD80 tumor eradication in 40% of mice (6). Although these data show a role for *in vivo* costimulation in tumor eradication by genetically modified

Authors' Affiliations: Departments of [1]Medicine and [2]Radiology; [3]Research Animal Resource Center; [4]Immunology Program; and [5]Gene Transfer and Somatic Cell Engineering Laboratory, Memorial Sloan Kettering Cancer Center, New York, New York

Received 3/23/07; revised 5/17/07; accepted 5/23/07.

Grant support: CA95152, CA59350, CA08748, CA86438, and CA96945; The Alliance for Cancer Gene Therapy (M. Sadelain); The Annual Terry Fox Run for Cancer Research (New York, NY) organized by the Canada Club of New York, William H. Goodwin and Alice Goodwin, and the Commonwealth Cancer Foundation for Research and the Experimental Therapeutics Center of Memorial Sloan Kettering Cancer Center (R.J. Brentjens and M. Sadelain); Amgen Career Development Award (R.J. Brentjens); and the Bocina Cancer Research Fund.

The costs of publication of this article were defrayed in part by the payment of page charges. This article must therefore be hereby marked *advertisement* in accordance with 18 U.S.C. Section 1734 solely to indicate this fact.

Requests for reprints: Renier J. Brentjens, Department of Medicine, Memorial Sloan Kettering Cancer Center, Box 242, 1275 York Avenue, New York, NY 10021. Phone: 212-639-7053; E-mail: brentjer@mskcc.org.

doi:10.1158/1078-0432.CCR-07-0674

tumor-targeted T cells, they neither fully explain the etiologies of treatment failure in a majority of treated mice nor provide a strategy to overcome these limitations.

To further investigate the *in vivo* limitations of this adoptive T-cell strategy, we chose to pursue the treatment of NALM-6 tumors in SCID-Beige mice due to the fact that the tumor in this model has several features that mimic B-cell ALL disease in human subjects: First, the disease is systemic; second, similar to the clinical setting, NALM-6 tumor displays an anatomic disease pattern that includes involvement of the bone marrow and central nervous system (CNS; ref. 7); and third, the NALM-6 tumor cell line fails to express costimulatory ligands as do most B-cell leukemias, including B-cell ALL. In this report, we use this NALM-6 tumor model to address the limitation of failed *in vivo* T-cell costimulation, and further investigate T-cell persistence and homing as potential etiologies of treatment failure. We found that both *in vivo* costimulation as well as repeated T-cell administration were critical to the complete eradication of NALM-6 tumor in SCID-Beige mice. Subsequent modifications in our treatment strategy based on these findings resulted in a markedly improved rate of complete tumor eradication in treated mice.

To our knowledge, this is the first report demonstrating complete eradication of a systemic human tumor lacking costimulatory ligands using genetically targeted T cells. Furthermore, complete eradication is achieved in the absence of further *in vivo* therapy, including prior chemotherapy or subsequent cytokine support. These optimized treatment strategies are likely to be applicable to future human trials enrolling patients with B-cell malignancies, including B-cell ALL.

Materials and Methods

Cell lines and T cells. Raji and NALM-6 tumor cell lines were cultured in RPMI 1640 (Life Technologies) supplemented with 10% heat-inactivated FCS, nonessential amino acids, HEPES buffer, pyruvate, and BME (Life Technologies). PG-13 and gpg29 retroviral producer cell lines were cultured in DMEM (Life Technologies) supplemented with 10% FCS, and NIH-3T3 artificial antigen-presenting cells (AAPC), described previously (6), were cultured in DMEM supplemented with 10% heat-inactivated donor calf serum. All media were supplemented with 2 mmol/L L-glutamine (Life Technologies), 100 units/mL penicillin, and 100 μg/mL streptomycin (Life Technologies). Where indicated, medium was supplemented with 10 ng/mL interleukin 15 (IL-15; R&D Systems).

Construction of second-generation CAR fusion genes. Construction of the 19z1 and Pz1 scFv-ζ chain fusion proteins have been previously published (6, 8). The resulting fusion genes were cloned into the SFG retroviral vector (9). VSV-G pseudotyped retroviral supernatants derived from transduced gpg29 fibroblasts were used to construct stable PG-13 gibbon ape leukemia virus (GaLV) envelope-pseudotyped retroviral producing cell lines using polybrene (Sigma) as described previously (8). All second-generation fusion receptors contain the scFv derived from 19z1. Human CD28, DAP10, 4-1BB, and OX40 coding regions were PCR amplified from a human activated T-cell cDNA library, and subcloned into the TopoTA PCR 2.1 cloning vector (Invitrogen). All receptor constructs were generated using overlapping PCR. The resulting cassettes were designed to facilitate the exchange of the transmembrane and signaling domains of the 19z1 construct by *Not*I/*Bam*HI restriction sites encoded in flanking primers.

Retroviral transduction and expansion of human T lymphocytes. Retroviral transduction of healthy donor T cells, obtained under institutional review board–approved protocol 90-095, is described elsewhere (8). For *ex vivo* expansion studies and cytokine release assays, transduced T cells were cocultured for 7 days after retroviral transduction in 24-well tissue culture plates (Falcon, Becton Dickinson) with confluent NIH 3T3 AAPCs in RPMI medium supplemented with 10% FCS, L-glutamine, streptomycin, and penicillin, with no added cytokines. For *in vivo* experiments, transduced T cells were injected after expansion on 3T3(CD19/CD80) or, for the $Pz1^+$ T cell control, 3T3[prostate-specific membrane antigen (PSMA)/CD80] AAPCs in RPMI medium as above, supplemented with 20 IU IL-2/mL and 10 ng/mL IL-15. For mice treated with multiple injections of modified T cells for 4 weeks, CAR^+ T cells were generated by weekly restimulation on AAPCs as described above.

Western blot analysis. Western blot analysis of T-cell lysates under reducing conditions with 0.1 mol/L DTT (Sigma) was done as previously described (10). Briefly, transduced T cells were washed in PBS and resuspended in radioimmunoprecipitation assay buffer (Boston Bioproducts) with mini complete protease inhibitor as per the manufacturer's instructions (Roche Diagnostics). Resulting proteins were separated on 12% SDS-PAGE mini gels (Bio-Rad) after the addition of 6× reducing loading buffer (Boston Bioproducts) and heating at 100°C for 10 min. Separated proteins were subsequently transferred to Immobilon membranes and probed using an anti-human CD3 ζ chain monoclonal antibody (BD Biosciences). Antibody binding was detected by probing the blot with goat anti-mouse horse radish peroxidase–conjugated antibody followed by luminescent detection using Western Lighting Chemiluminescence Reagent Plus (Perkin-Elmer Life Sciences) as per the manufacturer's instructions.

Cytotoxicity assays. We determined the cytotoxic activity of transduced T cells by standard ^{51}Cr release assays as described elsewhere (8). Briefly, transduced T cells were assessed by fluorescence-activated cell sorting analysis for CAR expression as well as CD4:CD8 ratio on day 4 after transduction. NALM-6 tumor cells were labeled with ^{51}Cr for 1 h at 37°C, washed with RPMI medium supplemented with 10% FCS, and resuspended in the same medium at a concentration of 1×10^5 tumor cells/mL. Transduced T cells were added to tumor cells at varying effector to target cell ratios in 96-well tissue culture plates in a final volume of 200 μL, and incubated for 4 h at 37°C. Thereafter, 30 μL of supernatant from each well was analyzed using Lumaplate-96 microplates (Packard Bioscience) by a Top Count NXT microplate scintillation counter (Packard Bioscience). Effector cell number in all assays was calculated based on the total number of $CD8^+$ CAR^+ T cells.

Cytokine detection assays. Cytokine assays were done per manufacturer's specifications using the multiplex Human Cytokine Detection System (Upstate, Inc.). Luminescence was assessed using the Luminex IS100 system and analyzed for cytokine concentration using IS 2.2 software (Luminex Corp.).

Flow cytometry. We did flow cytometry using a FACScan cytometer with Cellquest software (BD Biosciences). Cells were labeled with either phycoerythrin-conjugated, CAR-specific polyclonal goat antibody (Caltag Laboratories) or phycoerythrin-labeled anti-human CD8 and FITC-labeled anti-human CD4 monoclonal antibodies (Caltag Laboratories).

Retroviral transduction of NALM-6 tumor cells with GFP-FFLuc. The *GFP-FFLuc* gene (Clontech Laboratories) was subcloned into the SFG retroviral vector. VSV-G pseudotyped retroviral supernatants derived from gpg29 fibroblasts transduced with the resulting SFG (GFP-FFLuc) plasmid were used to transduce NALM-6 tumor cells as described elsewhere (10). Resulting tumor cells were sorted by fluorescence-activated cell sorting for GFP expression.

In vivo *SCID-Beige mouse tumor models.* We inoculated 8- to 12-week-old FOX CHASE C.B-17 (SCID-Beige) mice (Taconic) with tumor cells by tail vein injection. We subsequently treated mice by tail vein injection with transduced T cells. In the Raji tumor model, mice were injected by tail vein with 5×10^5 Raji tumor cells on day 1, and on day 6 were treated with a single i.v. dose of 1×10^7 CAR^+ T cells. In the NALM-6 upfront treatment tumor model, mice were injected by tail vein on day 1 with 1×10^6 NALM-6 tumor cells, and on days 2 to 4 were injected i.v. with 1×10^7 CAR^+ T cells daily. In the weekly

treatment model, mice were inoculated with NALM-6 tumor cells on day 1, and subsequently treated with i.v. injections of 1×10^7 CAR$^+$ T cells on days 2, 8, 15, and 22. In all experiments, mice that developed hind limb paralysis or decreased response to stimuli were sacrificed by CO_2 asphyxiation. All murine studies were done in the context of an Institutional Animal Care and Use Committee–approved protocol (no. 00-05-065).

In vivo *bioluminescence of NALM-6 tumors.* Bioluminescence imaging was done using Xenogen IVIS Imaging System (Xenogen) with Living Image software (Xenogen) for acquisition of imaging data sets. Mice were infused by i.p. injection with 150 mg/kg D-luciferin (Xenogen) suspended in 200 μL PBS. Ten minutes later, mice were imaged while under 2% isoflurane anesthesia. Image acquisition was done on a 15- or 25-cm field of view at medium binning level for 0.5- to 3-min exposure time. Both dorsal and ventral views were obtained on all animals. Tumor bulk, as determined by IVIS imaging, was assessed as described previously (11).

Histologic analysis of mouse tissue sections. Mouse tissues were fixed in 10% buffered formalin phosphate (Fisher Scientific). Osseous samples (head with brain, vertebral column with spinal cord, and hind limbs) were fixed and decalcified in SurgiPath Decalcifier I (SurgiPath Medical Industries) as per the manufacturer's specifications. All tissues were processed by routine methods and embedded in paraffin wax. Five-micrometer sections were stained with H&E (Poly Scientific).

Statistics. Statistical analysis of survival data by log-rank analysis was obtained using GB-STAT software (Dynamic Microsystems).

Results

Construction of second-generation costimulatory CARs. We have previously shown that T cells which express the first-generation 19z1 CAR successfully eradicate systemic CD80/CD86$^+$ Raji tumor in SCID-Beige mice. However, in the same report, we further show the inability of 19z1$^+$ T cells to fully eradicate systemic NALM-6 tumors, which fail to express the costimulatory CD80 and CD86 ligands. The genetic modification of NALM-6 tumors to express CD80 allowed for the complete eradication of tumor in a significant number of treated mice (6) consistent with the notion that *in vivo* T-cell costimulation enhances the antitumor efficacy of tumor-specific T cells.

Because most B-cell tumors fail to express costimulatory ligands, we addressed this limitation of our treatment strategy by constructing a series of second-generation CARs designed to deliver an additional costimulatory signal in the absence of exogenous costimulatory ligand by inserting the transmembrane and cytoplasmic signaling domains of the CD28, DAP10, and 4-1BB costimulatory receptors into the 19z1 CAR (Fig. 1A). Alternative DAP-10– and 4-1BB–containing receptors, as well as the OX-40–containing CAR, were designed to contain the CD8 transmembrane domain from the original 19z1

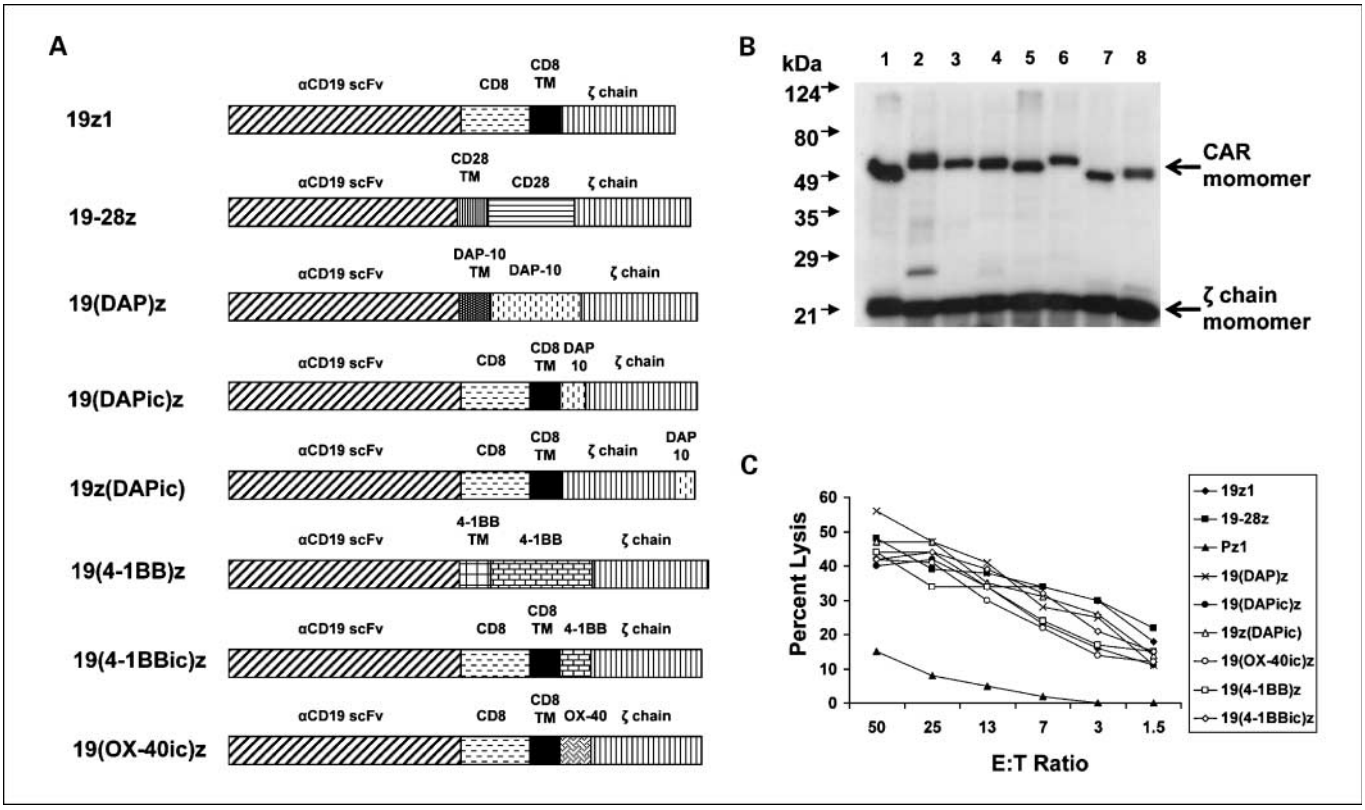

Fig. 1. T-cell expression of second-generation CARs. *A,* pictorial representations of 19z1 with second-generation CAR genes demonstrating the genetic fragments used to generate the costimulatory CARs. *B,* Western blot analysis of T cells retrovirally transduced with CAR genes under reducing conditions. Membranes were probed with a monoclonal antibody specific to the cytoplasmic domain of the human ζ chain and show the expression of CARs at the expected molecular weights. The native T-cell ζ chain is indicated. Lane 1, 19z1; lane 2, 19-28z; lane 3, 19(DAPic)z; lane 4, 19z(DAPic); lane 5, 19(DAP)z; lane 6, 19(4-1BBic)z; lane 7, 19(4-1BB)z; and lane 8, 19(OX-40ic)z. *C,* NALM-6 tumor lysis by CAR$^+$ T cells was assessed by standard 4 h ^{51}Cr release assays. All T cells expressing CD19-targeted second-generation CARs lysed target tumor cells equally well when compared with T cells expressing the first-generation 19z1 CAR. Control T cells expressing the irrelevant Pz1 CAR did not significantly lyse NALM-6 tumors. Effector to target ratios (*E:T Ratio*) represent T cells normalized to the CD8$^+$ CAR$^+$ T-cell fraction. Data represent one of three different experiments using three different healthy donor T-cell populations with similar results.

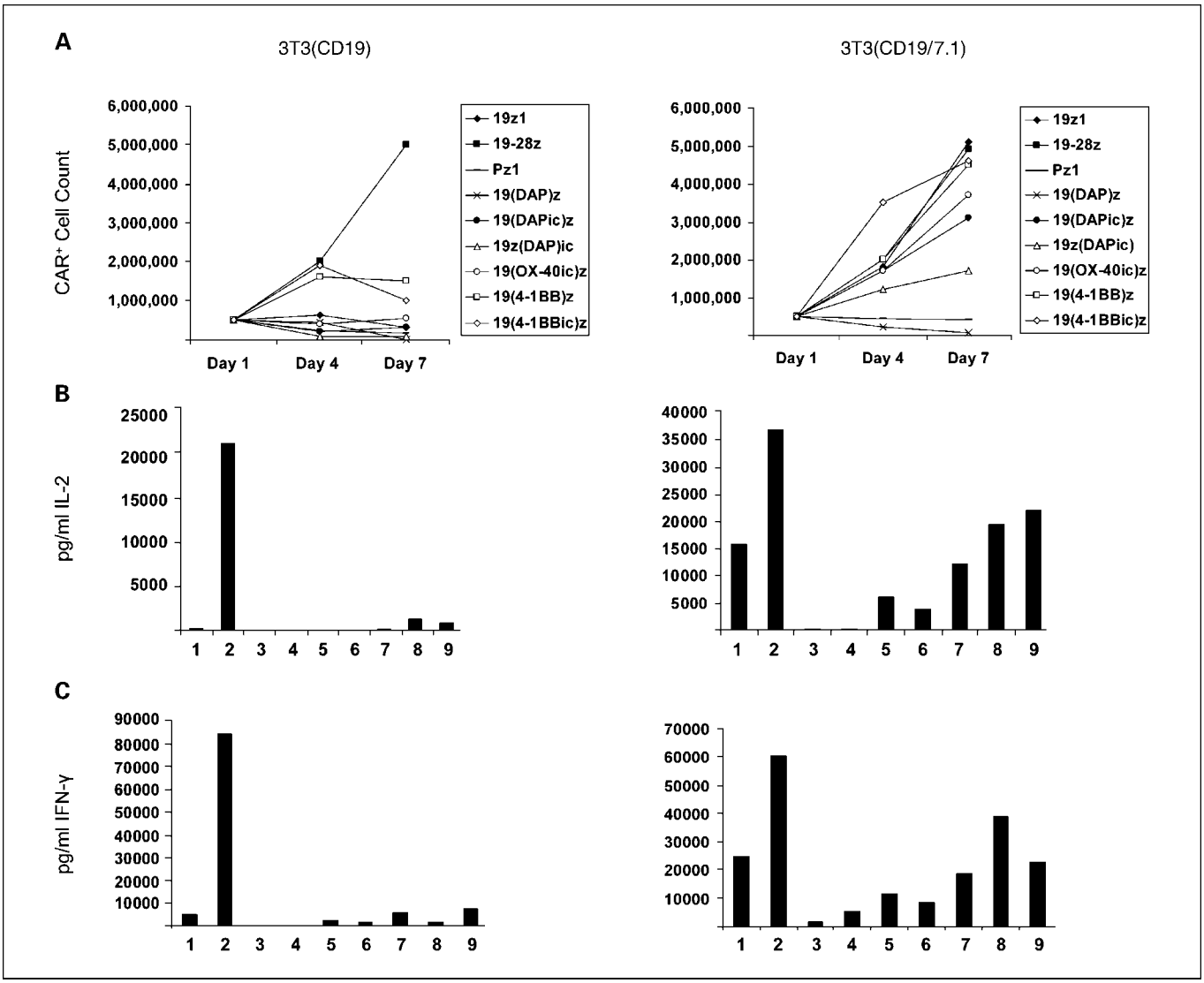

Fig. 2. *In vitro* T-cell costimulation of CAR$^+$ T cells as assessed by proliferation and cytokine secretion after coculture on NIH 3T3 fibroblast AAPCs. *A,* CAR-transduced T cells, normalized to the CAR$^+$ T-cell fraction, were cocultured on AAPC monolayers either without exogenous costimulation [3T3(CD19); *left*], or with exogenous costimulation [3T3(CD19/CD80); *right*]. On day 1, 5×10^5 CAR$^+$ T cells were cocultured on AAPC monolayers in 24-well tissue culture plates in cytokine-free medium. On days 4 and 7, total viable T-cell counts were obtained by trypan blue exclusion assays, and FACS analysis was done on these samples to calculate the total number of CAR$^+$ T cells. Whereas 19-28z, 19(4-1BB)z, and 19(4-1BBic)z transduced T cells expanded by day 4, only 19-28z$^+$ T cells continued to expand in the absence of exogenous CD80 costimulation (*left*). Control Pz1$^+$ T cells failed to expand in either setting. *B* and *C,* equal numbers of CAR$^+$ T cells were incubated in the absence of additional cytokines AAPC monolayers. Cell-free tissue culture supernatants were analyzed at 24 h after coculture for the presence of cytokines: lane 1, 19z1; lane 2, 19-28z; lane 3, Pz1; lane 4, 19(DAP)z; lane 5, 19(DAPic)z; lane 6, 19z(DAPic); lane 7, 19(OX-40ic)z; lane 8, 19(4-1BB)z; and lane 9, 19(4-1BBic)z. Only T cells that expressed the 19-28z CAR secreted significant levels of IL-2 (*B*) and IFNγ (*C*) in the absence of exogenous CD80. These data are representative of one of three different experiments using three different healthy donor T-cell populations, all of which showed the same proliferation and cytokine secretion patterns.

construct to assess whether this CAR design could enhance costimulatory signaling. Finally, we also assessed whether placing the DAP-10 signaling domain either proximal or distal to the ζ chain signaling domain improved CAR function.

T cells from healthy human donors were retrovirally transduced to express these CAR constructs. T-cell transduction efficiency, as assessed by flow cytometric analysis, ranged from 50% to 80% (data not shown). Western blot analysis of transduced T cells, normalized to the CAR$^+$ fraction, showed comparable levels of CAR proteins present at the predicted molecular weights (Fig. 1B).

To verify that second-generation CARs when expressed in human T cells retained the ability to lyse CD19$^+$ tumor cells *in vitro*, we conducted standard 4 h ^{51}Cr release assays using transduced healthy donor T cells targeting ^{51}Cr-labeled CD19$^+$ NALM-6 tumor cells (Fig. 1C). Effector to target ratio between different CAR constructs was normalized to the CD8$^+$ CAR$^+$ T-cell population. All tested CARs, with the exception of the Pz1$^+$ T-cell control, specific to the PSMA, were able to mediate tumor cell lysis equally well when compared with the first-generation 19z1 CAR.

Characterization of second-generation CAR costimulatory function. We have previously generated a series of AAPCs derived from NIH-3T3 murine fibroblasts genetically engineered to express either CD19 alone [3T3(CD19)] or both CD19 and CD80 [3T3(CD19/CD80); ref. 6]. When cocultured

with CD19-specific CAR$^+$ T cells, the former [3T3(CD19)] provides T cells with a CAR-mediated activation signal (signal 1) alone, whereas the latter [3T3(CD19/CD80)] provides T cells with signal 1 as well as an exogenous costimulatory signal (signal 2) mediated through CD80 on the AAPC binding to CD28 on the T cell.

To assess CAR-mediated T-cell proliferation, transduced T cells were cocultured on both 3T3(CD19) and 3T3(CD19/CD80) AAPCs in the absence of exogenous cytokine. CAR$^+$ T-cell number was determined after coculture on 3T3(CD19) and 3T3(CD19/CD80) AAPCs (Fig. 2A) on days 4 and 7. Following coculture on 3T3(CD19) AAPCs, only T cells transduced with the 19-28z, 19(4-1BB)z, and 19(4-1BBic)z CARs expanded after 4 days of coculture, whereas at day 7, only T cells transduced with the 19-28z CAR had undergone significant proliferation (10-fold expansion) consistent with CAR-mediated T-cell costimulation. All other constructs failed to promote T-cell proliferation in the absence of exogenous costimulation. Significantly, 19-28z CAR$^+$ T cells proliferated equally well on either 3T3(CD19) or 3T3(CD19/CD80) AAPCs, and proliferated equally well when compared with 19z1$^+$ T cells in the setting of 3T3(CD19/CD80) AAPC stimulation.

We next assessed CAR$^+$ T-cell secretion of IL-2 and IFN-γ as surrogate makers of costimulation. Equal numbers of CAR$^+$ T cells with similar CD4:CD8 ratios were cocultured on 3T3(CD19) and 3T3(CD19/CD80) AAPCs in cytokine-free medium after initial T-cell transduction. At 24 h after T-cell coculture on AAPCs, tissue culture supernatants were analyzed for the presence of IL-2 and IFN-γ. Coculture of 19-28z$^+$ T cells on 3T3(CD19) AAPCs resulted in significantly elevated levels of IL-2 (Fig. 2B) and IFN-γ (Fig. 2C) when compared with the first-generation 19z1 CAR as well as the other six tested second-generation CARs. These data further confirm the ability of the 19-28z CAR to elicit a costimulatory signal independent of exogenous costimulatory ligand. Significantly, 4-1BB and DAP-10 constructs containing either the native or CD8 transmembrane domains showed no significant differences in function, and in the setting of the DAP-10 constructs, no differences in function were observed when the signaling domain was placed either proximal or distal to the ζ chain.

In vivo ***antitumor activity of alternative costimulatory CARs.*** To define the *in vivo* costimulatory activity of the 19-28z CAR, we initially compared the antitumor activity of 19z1$^+$ and 19-28z$^+$ T cells in a previously established systemic Raji tumor model. Because both 19z1$^+$ T cells and 19-28z$^+$ T cells are costimulated *in vivo* by CD80/CD86$^+$ Raji tumor cells, we predicted and observed equal long-term survival (50%) in both treatment groups (Fig. 3A). We next compared the same treatment groups (19z1 versus 19-28z) in mice bearing systemic NALM-6 tumor, which fails to express the CD80 and CD86 costimulatory ligands. We observed improved antitumor efficacy in the 19-28z treatment group (Fig. 3B). However, the improved long-term overall survival was modest (0 of 15 19z1$^+$ T cell–treated mice versus 3 of 17 or 18% of 19-28z$^+$ T cell–treated mice; $P < 0.03$). Treatment with 19(4-1BB)z$^+$ and 19(4-1BBic)z$^+$ T cells enhanced survival when compared with mice treated with the control Pz1$^+$ T cells, but overall survival was similar to 19z1$^+$ T cell–treated mice, with no long-term surviving mice (data not shown). Fluorescence-activated cell sorting analysis of single-cell suspensions of tissues derived from mice that failed 19-28z$^+$ T cell treatment showed persistent expression of CD19 on the tumor cells, ruling out the possibility that down-regulation of the CD19 target antigen was a source of treatment failure (data not shown).

Repeated administration of CD19-targeted T cells enhances complete NALM-6 tumor eradication. Using bioluminescent imaging of treated SCID-Beige mice bearing NALM-6(GFP-FFLuc) tumors, we found a 10- to 14-day delay of tumor progression after 19z1$^+$ T-cell therapy when compared with Pz1$^+$ T-cell therapy (Fig. 4A-B). A similar delay of tumor progression was seen after 19-28z$^+$ T-cell therapy in mice with relapsed disease (data not shown). Fluorescence-activated cell sorting analysis of single-cell suspensions derived from tissues of 19-28z$^+$ T cell–treated tumor-bearing mice confirmed a

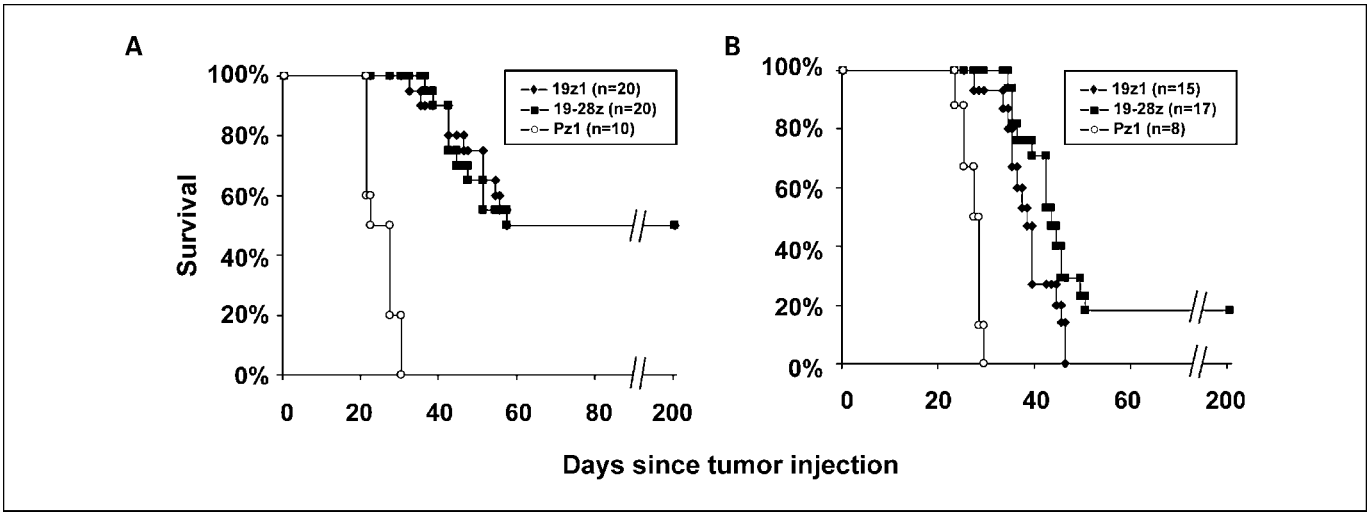

Fig. 3. *In vivo* analysis of CD19-specific CAR$^+$ T cells in SCID-Beige mice bearing systemic human CD19$^+$ tumors. *A,* treatment with 19z1$^+$ or 19-28z$^+$ T cells eradicated systemic Raji tumors in SCID-Beige mice equally well. Briefly, mice were injected by tail vein with 5×10^5 Raji tumor cells on day 1. Mice were subsequently treated with a single dose of 1×10^7 CAR$^+$ T cells by tail vein injection on day 6. Mice treated with either 19z1$^+$ or 19-28z$^+$ T cells eradicated tumor equally well with an overall 50% long-term survival in both treatment groups. *B,* treatment of NALM-6 bearing SCID-Beige mice with 19-28z$^+$ T cells (1×10^7 CAR$^+$ T cells injected daily $\times$ 3 d) statistically enhanced survival when compared with similar treatment with 19z1$^+$ T cells (18% versus 0% long-term survival; $P < 0.03$).

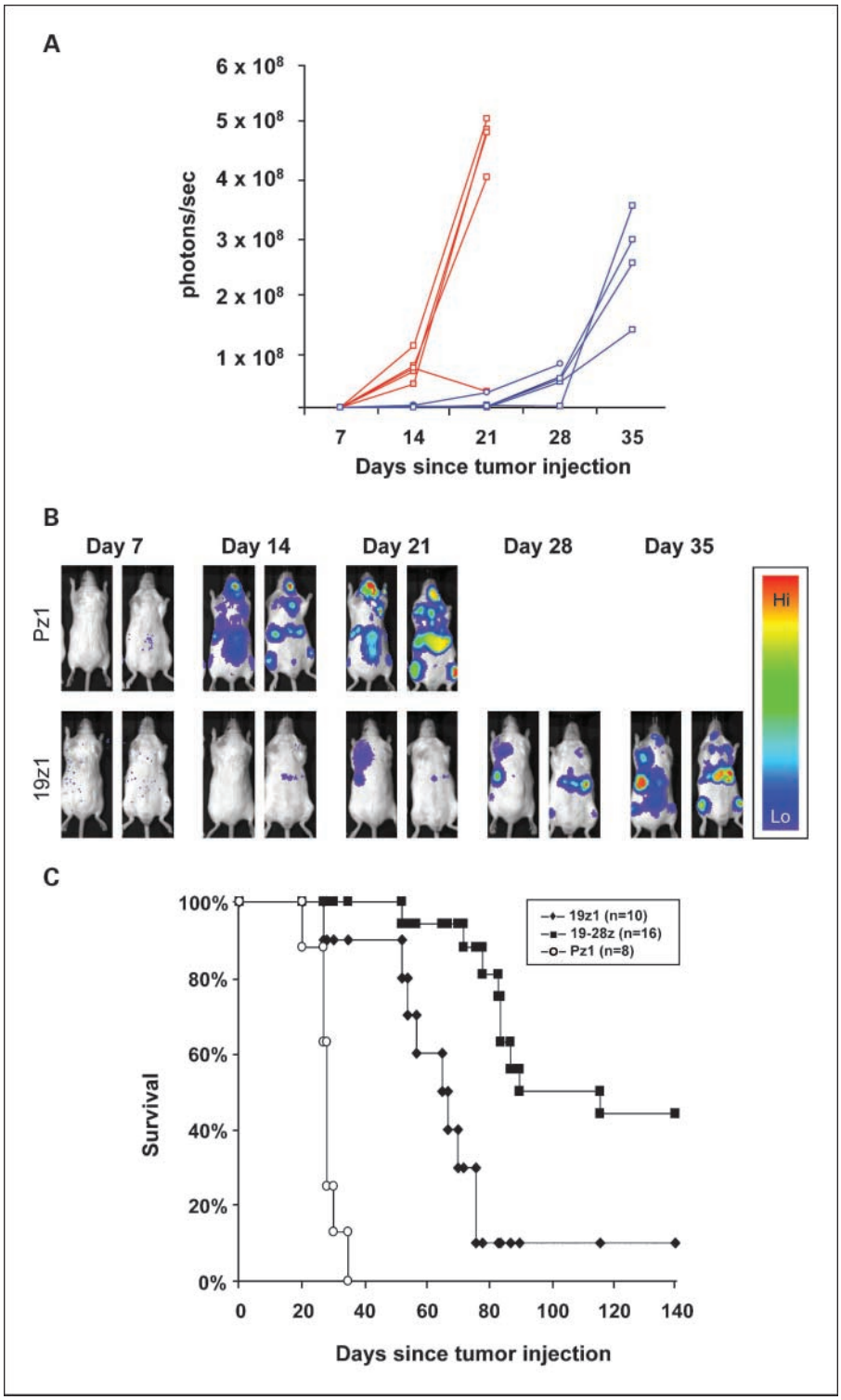

Fig. 4. Enhanced antitumor activity through weekly CD19-targeted T-cell infusions. *A,* treatment of NALM-6 tumor-bearing mice with daily targeted T-cell injections on days 1 to 3 after tumor cell injection delays tumor growth for 10 to 14 d as assessed by analysis of IVIS images of mice treated with either 19z1$^+$ T cells or the control Pz1$^+$ T cells. NALM-6 (GFP-Luc) tumor burden was assessed based on ventral mouse images in photons per second emitted after luciferin injection. Similar data were obtained in mice treated with 19-28z$^+$ T cell – treated mice (not shown). *B,* representative dorsal and ventral images of NALM-6 (GFP-Luc) – bearing mice obtained weekly after T-cell therapy shows delayed tumor growth in 19z1$^+$ T cell – treated mice when compared with the Pz1$^+$ T-cell control mice. *C,* weekly 19-28z$^+$ T cell tail vein injection for 4 wks on days 2, 9, 16, and 22, after NALM-6 tumor injection on day 1, enhanced long-term survival of treated mice >4-fold (44% versus 10%) when compared with similar treatment with either 19z1$^+$ T cells ($P < 0.002$) or the control Pz1$^+$ T cell – treated mice. Results represent pooled data from two separate experiments.

short *in vivo* T-cell survival (data not shown), consistent with previously published data demonstrating limited *in vivo* survival of human T cells in an immunocompromised murine host (11 – 14).

To assess whether enhanced *in vivo* T-cell persistence promoted long-term survival, we generated a sustained *in vivo* population of tumor-targeted T cells in NALM-6 tumor bearing SCID-Beige mice by injecting CAR$^+$ T cells weekly for 4 weeks. The incidence of long-term survival with 19-28z$^+$ T-cell therapy increased from 18% as seen in the upfront daily ×3 treatment schedule to 44% in the weekly treatment schedule (Figs. 3B and 4C, respectively). Consistent with an additive effect of *in vivo* T-cell persistence and costimulation, we found superior antitumor activity of 19-28z$^+$ T cells, when compared with

19z1$^+$ T cells, as shown by 44% versus 10% long-term survival ($P < 0.002$), using this weekly T-cell dosing schedule (Fig. 4C).

CD19-targeted T cells eradicate NALM-6 tumor cells at disparate anatomic sites in SCID-Beige mice after adoptive T-cell therapy. Despite improved survival with the weekly T-cell dosing treatment schedule, 56% of 19-28$^+$ T cell–treated mice ultimately failed therapy. To assess whether these mice developed persistent or recurrent tumor in consistent anatomic sites potentially restricted from T-cell penetration or detection, we monitored *in vivo* NALM-6(GFP-FFLuc) tumor progression by weekly bioluminescent (IVIS) imaging in the setting of the weekly T-cell treatment regimen. In these studies, all control mice treated weekly with Pz1$^+$ T cells showed diffuse tumor progression at multiple sites over the treatment period (Fig. 5A). By weekly IVIS monitoring of the 19z1$^+$ T cell–treated mice, 40% (4 of 10) had no detectable disease upon completion of therapy (day 28). In the nine mice that developed progressive disease in this treatment group, initial disease persistence or relapse was noted at distinct anatomic sites in different mice, including the bone marrow ($n = 2$; Fig. 5B), the periodontal region ($n = 3$), the spleen/calvarium ($n = 1$), the abdomen ($n = 1$), and the CNS/calvarium ($n = 1$). Overall, 69% (11 of 16) of mice treated with weekly 19-28z$^+$ T-cell infusions showed no evidence of disease by weekly IVIS imaging upon completion of therapy. The 56% (9 of 16) of 19-28z$^+$ T cell–treated mice, which ultimately failed therapy, likewise showed detectable disease at disparate anatomic sites, including the spleen ($n = 1$; Fig. 5C), the CNS/calvarium ($n = 2$; Fig. 5D), the periodontal region ($n = 4$; Fig. 5E), and the bone marrow ($n = 2$; Fig. 5F). Significantly, persistent disease in the periodontal region, despite ongoing T-cell therapy, was noted in 30% of 19z1-treated mice, and 25% of 19-28z–treated mice, accounting for a large majority of the mice with evidence of disease upon completion of treatment. The presence of tumor as assessed by bioluminescent imaging in 19-28z$^+$ T cell–treated mice was subsequently confirmed by histologic analysis, demonstrating NALM-6 tumor infiltration in the bone marrow (Fig. 6A-B), the spleen (Fig. 6C-D), and the periodontal region (Fig. 6E-F).

Discussion

The successful clinical application of adoptive therapy of cancer with genetically targeted T cells requires both a better understanding of the *in vivo* biology of genetically modified T cells, as well as innovative means of enhancing the *in vivo* potency of these T cells. In this report, we use the clinically relevant NALM-6 systemic murine model of human B-cell ALL, which involves the bone marrow and CNS, and lacks

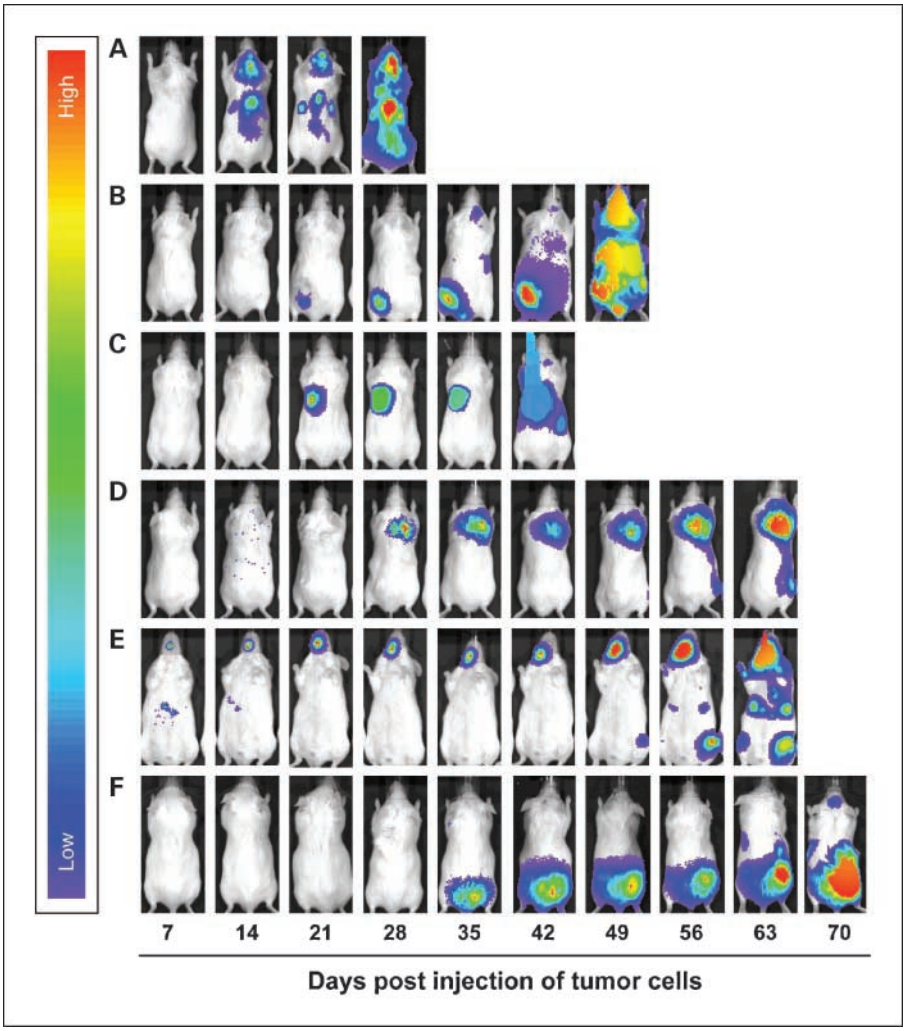

Fig. 5. Bioluminescent imaging of NALM-6(GFP-FFLuc) tumor cells after weekly CAR$^+$ T-cell treatment for 4 wks. Weekly treatment with Pz1$^+$ T cells in mice bearing systemic NALM-6 (GFP-FFLuc) resulted in a typical diffuse pattern of tumor cell expansion involving the bone marrow, spleen, liver, lymph nodes, and periodontal regions (*A*). All mice developed lethal disease 4 to 5 wks after tumor cell injection. Mice treated weekly with 19z1$^+$ T cells showed persistent or relapsed disease at distinct anatomic sites including the bone marrow (*B*), periodontal region, CNS/calvarium, abdomen, and spleen (data not shown). Treatment failure in 19-28z$^+$ T cell – treated mice likewise occurred at distinct but disparate anatomic sites including the spleen (*C*), CNS/calvarium (*D*), periodontal region (*E*), and bone marrow (*F*).

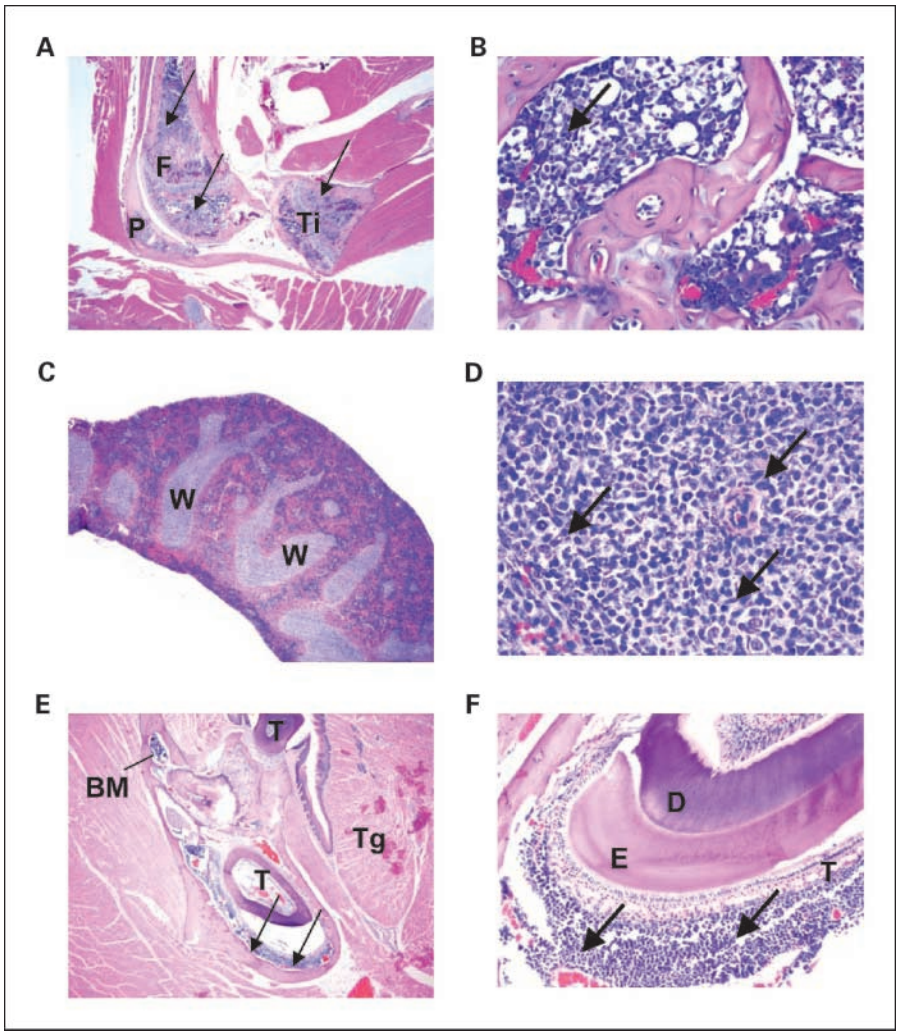

Fig. 6. Histologic analysis of tissue sections of sacrificed mice with evidence of tumor by IVIS imaging. To validate the presence of NALM-6 (GFP-FFLuc) tumor in various tissues as assessed by IVIS imaging, several mice were sacrificed and tissues from these mice were analyzed histologically for the presence of tumor. *A,* low-magnification photomicrograph of the hind leg showing femur (*F*), tibia (*Ti*), and patella (*P*) infiltrated by NALM-6 (GFP-FFLuc) tumor cells (*arrows*). *B,* high-magnification photomicrograph of the femur showing diffuse tumor infiltration. *C,* low-magnification photomicrograph of a mouse spleen demonstrating abnormally expanded white pulp (*W*) due to tumor infiltration. *D,* higher-magnification photomicrograph of the white pulp shows atypical lymphocytes and scattered mitotic figures consistent with tumor infiltration. *E,* low-magnification photomicrograph of a coronal section through the head showing mandibular bone marrow (*BM*) free of tumor, tongue (*Tg*), and a tooth (*T*) surrounded by NALM-6 (GFP-FFLuc) tumor cells (*arrows*) in a mouse with periodontal disease as assessed by IVIS imaging. *F,* higher-magnification photomicrograph showing tumor between the bone (*B*) and the enamel (*E*) and dentin (*D*) of the tooth (*arrows*). The tooth pulp in this mouse was not infiltrated with tumor.

expression of costimulatory ligands, features common to human pre–B-cell leukemia. Using this model, we studied *in vivo* T-cell function by assessing the roles of costimulation, persistence, and homing in the successful eradication of systemic disease.

CD3 ζ chain signaling through either the native TCR or a first-generation CAR results in an initial T-cell activation termed signal 1. For subsequent proliferation to occur, a costimulatory signal, or signal 2, is often required, which is mediated through the binding of costimulatory receptors expressed by the T cell to cognate costimulatory ligands expressed on the APC or target cell (15–18). We have previously shown that NALM-6 tumors genetically engineered to express the CD80 costimulatory ligand enhanced complete tumor eradication in mice treated with the first-generation 19z1 CAR (6). Although signal 1 alone is capable of triggering T cell–mediated cytolysis and is sufficient to eradicate tumor in the setting of suitably high numbers of adoptively transferred T cells (11), the generation of the large T cell numbers required to achieve complete tumor eradication with T cells that express first-generation CARs is less practical in the clinical setting. Therefore, because most tumors fail to express costimulatory ligands, successful application of this treatment approach has required the development of second-generation CARs capable of delivering both primary as well as costimulatory signals to the modified T cell upon engagement with the targeted tumor antigen (12–14, 19–24).

To address this limitation, we constructed a series of second-generation CARs containing the cytoplasmic signaling domains of known T-cell costimulatory receptors, which mediate IL-2 secretion, including CD28 (25), DAP-10 (26, 27), OX-40 (28), and 4-1BB (16, 29). Our studies presented here show that of these signaling domains, only the inclusion of the CD28 transmembrane and signaling domains into the 19z1 CAR enhanced both T-cell proliferation and cytokine secretion *in vitro* in the absence of exogenous costimulatory ligands. These data are consistent with the ability of the 19-28z receptor to provide both primary and costimulatory signals to the T cell.

Several groups have previously published data on the *in vitro* activity of human T cells modified with various second-generation CARs (19–22, 24, 30). The *in vitro* data presented here are consistent with previously published studies investigating the ability of CARs containing the CD28 cytoplasmic domain to costimulate T cells independent of exogenous costimulation. Discrepancies between our findings and those published by others demonstrating enhanced costimulation in second-generation CARs bearing the cytoplasmic signaling domains of the 4-1BB and OX-40 receptors (21, 22) may be due to both differences in target antigen and CAR construction,

implying a critical role of extracellular CAR design to signaling function (31). Significantly, modification of 4-1BB and DAP-10 CAR constructs by either altering the transmembrane domain or the location of the DAP10 costimulatory signaling domain failed to enhance CAR function. More recently, other investigators have published promising *in vitro* data describing "third-generation" CARs, which incorporate the cytoplasmic domains of other T-cell signaling ligands in CD28-containing second-generation CARs including OX-40 (24) and Lck (32). However, to date, no *in vivo* data has been published using these constructs.

Although we and others have previously published data on the *in vitro* activity of human T cells modified with various second-generation CARs, few have explored the activity of these modified T cells *in vivo* (12–14, 23). To date, only two studies have directly compared the activity of T cells transduced with a first-generation CAR to T cells expressing a second-generation CAR. Teng et al. (13) used a s.c. murine tumor model that showed improved antitumor activity after treatment with a CD28-containing CAR when compared with a first-generation CAR, but failed to show complete tumor eradication with T cells expressing either construct. More recently, Kowolik et al. (33) compared first to second-generation CD19-targeted CAR^+ T cells using an i.p. $CD19^+$ $CD80/86^+$ Burkitt lymphoma (Daudi) tumor model. These studies likewise showed superior *in vivo* antitumor efficacy of CD28-containing CAR^+ T cells when compared with the first-generation CD19-targeted CAR^+ T cells.

Here, we have furthered the analysis of CD28-containing CARs by demonstrating enhanced antitumor activity of human T cells bearing the 19-28z CAR, compared side by side to the 19z1 CAR, in a clinically relevant systemic, $CD19^+$ $CD80/CD86^-$ ALL SCID-Beige tumor model. For the first time, our studies show the ability of genetically targeted T cells to fully eradicate systemic tumor cells devoid of costimulatory ligands, even in the absence of *in vivo* cytokine support. We found that mice bearing systemic NALM-6 tumors treated with T cells transduced to express the second-generation 19-28z CAR had significantly enhanced survival when compared with mice treated with $19z1^+$ T cells. However, this improved long-term survival was modest (Fig. 3B). We postulated that treatment failure in this model was due to overall poor *in vivo* survival of human T cells in the SCID-Beige mouse. Consistent with the notion that *in vivo* modified T-cell persistence is critical to the complete eradication of tumor, we found that further prolonging T-cell presence in tumor bearing mice through weekly injections of modified T cells delayed tumor progression in both $19z1^+$ and $19\text{-}28z^+$ T cell–treated mice (Fig. 4C). This modified treatment strategy markedly improved the long-term survival of $19\text{-}28z^+$ T cell–treated mice when compared with the upfront $19\text{-}28z^+$ T-cell treatment schema (Figs. 3B and 4C). Our modified treatment strategy further highlights the additional significance of *in vivo* costimulation in tumor eradication as shown by the improved long-term survival of mice treated with weekly infusions of $19\text{-}28z^+$ T cells when compared with mice treated with weekly infusions of $19z1^+$ T cells. The exact mechanism(s) whereby 19-28z CAR signaling enhances T-cell antitumor activity remains speculative. Although *in vivo* costimulation through the 19-28z CAR may enhance T-cell survival, enhanced antitumor activity may also be due to superior *in vivo* proliferation. Alternatively, costimulatory signaling through the 19-28z CAR may avert T-cell anergy, allowing for the improved serial killing of tumor cells by each T cell. Further studies are needed to better elucidate these potential mechanisms.

Using IVIS bioluminescent imaging, we found that a majority of mice that failed therapy had no detectable evidence of tumor after the completion of weekly T-cell therapy, but only thereafter relapsed at various anatomic sites, including the bone marrow, the spleen, periodontal area, and the CNS/calvarium (Fig. 5). In light of the disparate patterns of disease relapse after treatment, these data are consistent with the notion that modified T cells successfully home to multiple sites of tumor involvement. Furthermore, given the fact that tumor relapse occurred in the majority of mice only upon cessation of therapy, our data suggests that treatment failure in this tumor model may be attributable, in part, to a suboptimal duration of T-cell therapy. Finally, although our data support the notion of successful homing of CAR-modified T cells to systemic anatomic sites in the setting of a hematologic malignancy, it remains to be seen if similar successful homing of CAR-modified T cells occurs in the setting of solid tumor metastases.

One anatomic exception to successful T-cell homing is in the periodontal region where persistent disease was noted in 30% of weekly $19z1^+$ T cell and 25% of weekly $19\text{-}28z^+$ T-cell treated mice despite ongoing therapy. Interestingly, periodontal tumor infiltration in a xenograft model of the PC-3 human prostate cancer cell line has been previously reported and attributed by the authors of this study to the proliferative microenvironment generated by mouse incisors, which continuously erupt (34). Because the periodontal region is not a common site of ALL or prostate cancer relapse in the clinical setting, the significance of this finding is less likely to be clinically relevant, and more likely to be a peculiarity of xenogeneic murine tumor models.

In conclusion, the data presented here have several potential implications for the use of adoptive immunotherapy using genetically targeted T cells in cancer therapy. First, the data show superior *in vivo* antitumor activity of T cells modified to express a CD28-containing costimulatory second-generation CAR in the setting of tumor cells, which fail to express costimulatory ligands. Second, our findings strongly support the view that *in vivo* T-cell persistence is critical to the successful application of this treatment strategy. Third, our data show that engineered T cells successfully home to multiple systemic sites of tumor involvement and is therefore an unlikely source of treatment failure in most mice. Finally, these studies support the continued use of xenogeneic tumor models in the study of *in vivo* human T-cell biology after adoptive therapy.

Based on these and other (6) preclinical findings, we are planning to conduct a clinical trial treating chemotherapy-refractory chronic lymphocytic leukemia patients with autologous $19\text{-}28z^+$ T cells. Furthermore, the significance of T-cell persistence as shown here predicts that repeated T-cell infusions in the setting of poor *in vivo* T-cell survival will likely enhance the therapeutic efficacy of this treatment strategy, a hypothesis we plan to address in subsequent clinical trials.

Acknowledgments

We thank Ellin Berman for her thoughtful advice and critical review of the manuscript.

References

1. Sadelain M, Riviere I, Brentjens R. Targeting tumours with genetically enhanced T lymphocytes. Nat Rev Cancer 2003;3:35–45.

2. Baxevanis CN, Papamichail M. Targeting of tumor cells by lymphocytes engineered to express chimeric receptor genes. Cancer Immunol Immunother 2004; 53:893–903.

3. Rossig C, Brenner MK. Genetic modification of T lymphocytes for adoptive immunotherapy. Mol Ther 2004;10:5–18.

4. Dotti G, Heslop HE. Current status of genetic modification of T cells for cancer treatment. Cytotherapy 2005;7:262–72.

5. Mansoor W, Gilham DE, Thistlethwaite FC, Hawkins RE. Engineering T cells for cancer therapy. Br J Cancer 2005;93:1085–91.

6. Brentjens RJ, Latouche JB, Santos E, et al. Eradication of systemic B-cell tumors by genetically targeted human T lymphocytes co-stimulated by CD80 and interleukin-15. Nat Med 2003;9:279–86.

7. Gunther R, Chelstrom LM, Tuel-Ahlgren L, Simon J, Myers DE, Uckun FM. Biotherapy for xenografted human central nervous system leukemia in mice with severe combined immunodeficiency using B43 (anti-CD19)-pokeweed antiviral protein immunotoxin. Blood 1995;85:2537–45.

8. Gong MC, Latouche JB, Krause A, Heston WDW, Bander NH, Sadelain M. Cancer patient T cells genetically targeted to prostate-specific membrane antigen specifically lyse prostate cancer cells and release cytokines in response to prostate-specific membrane antigen. Neoplasia 1999;1:123–7.

9. Riviere I, Brose K, Mulligan RC. Effects of retroviral vector design on expression of human adenosine deaminase in murine bone marrow transplant recipients engrafted with genetically modified cells. Proc Natl Acad Sci U S A 1995;92:6733–7.

10. Latouche JB, Sadelain M. Induction of human cytotoxic T lymphocytes by artificial antigen-presenting cells. Nat Biotechnol 2000;18:405–9.

11. Gade TP, Hassen W, Santos E, et al. Targeted elimination of prostate cancer by genetically directed human T lymphocytes. Cancer Res 2005;65: 9080–8.

12. Pinthus JH, Waks T, Malina V, et al. Adoptive immunotherapy of prostate cancer bone lesions using redirected effector lymphocytes. J Clin Invest 2004;114: 1774–81.

13. Teng MW, Kershaw MH, Moeller M, Smyth MJ, Darcy PK. Immunotherapy of cancer using systemically delivered gene-modified human T lymphocytes. Hum Gene Ther 2004;15:699–708.

14. Westwood JA, Smyth MJ, Teng MW, et al. Adoptive transfer of T cells modified with a humanized chimeric receptor gene inhibits growth of Lewis-Y-expressing tumors in mice. Proc Natl Acad Sci U S A 2005;102: 19051–6.

15. Liebowitz DN, Lee KP, June CH. Costimulatory approaches to adoptive immunotherapy. Curr Opin Oncol 1998;10:533–41.

16. Croft M. Co-stimulatory members of the TNFR family: keys to effective T-cell immunity? Nat Rev Immunol 2003;3:609–20.

17. Croft M. Costimulation of T cells by OX40, 4-1BB, and CD27. Cytokine Growth Factor Rev 2003;14: 265–73.

18. Riley JL, June CH. The CD28 family: a T-cell rheostat for therapeutic control of T-cell activation. Blood 2005;105:13–21.

19. Hombach A, Wieczarkowiecz A, Marquardt T, et al. Tumor-specific T cell activation by recombinant immunoreceptors: CD3 ζ signaling and CD28 costimulation are simultaneously required for efficient IL-2 secretion and can be integrated into one combined CD28/CD3 ζ signaling receptor molecule. J Immunol 2001;167: 6123–31.

20. Maher J, Brentjens RJ, Gunset G, Riviere I, Sadelain M. Human T-lymphocyte cytotoxicity and proliferation directed by a single chimeric TCRζ /CD28 receptor. Nat Biotechnol 2002;20:70–5.

21. Imai C, Mihara K, Andreansky M, et al. Chimeric receptors with 4-1BB signaling capacity provoke potent cytotoxicity against acute lymphoblastic leukemia. Leukemia 2004;18:676–84.

22. Finney HM, Akbar AN, Lawson AD. Activation of resting human primary T cells with chimeric receptors: costimulation from CD28, inducible costimulator, CD134, and CD137 in series with signals from the TCR ζ chain. J Immunol 2004;172:104–13.

23. Gyobu H, Tsuji T, Suzuki Y, et al. Generation and targeting of human tumor-specific Tc1 and Th1 cells transduced with a lentivirus containing a chimeric immunoglobulin T-cell receptor. Cancer Res 2004;64: 1490–5.

24. Pule MA, Straathof KC, Dotti G, Heslop HE, Rooney CM, Brenner MK. A chimeric T cell antigen receptor that augments cytokine release and supports clonal expansion of primary human T cells. Mol Ther 2005; 12:933–41.

25. Sharpe AH, Freeman GJ. The B7-28 superfamily. Nat Rev Immunol 2002;2:116–26.

26. Wu J, Song Y, Bakker AB, et al. An activating immunoreceptor complex formed by NKG2D and DAP10. Science 1999;285:730–2.

27. Diefenbach A, Tomasello E, Lucas M, et al. Selective associations with signaling proteins determine stimulatory versus costimulatory activity of NKG2D. Nat Immunol 2002;3:1142–9.

28. Mestas J, Crampton SP, Hori T, Hughes CC. Endothelial cell co-stimulation through OX40 augments and prolongs T cell cytokine synthesis by stabilization of cytokine mRNA. Int Immunol 2005;17:737–47.

29. Cannons JL, Lau P, Ghumman B, et al. 4-1BB ligand induces cell division, sustains survival, and enhances effector function of CD4 and CD8 T cells with similar efficacy. J Immunol 2001;167:1313–24.

30. Finney HM, Lawson AD, Bebbington CR, Weir AN. Chimeric receptors providing both primary and costimulatory signaling in T cells from a single gene product. J Immunol 1998;161:2791–7.

31. Guest RD, Hawkins RE, Kirillova N, et al. The role of extracellular spacer regions in the optimal design of chimeric immune receptors: evaluation of four different scFvs and antigens. J Immunother 2005;28: 203–11.

32. Geiger TL, Nguyen P, Leitenberg D, Flavell RA. Integrated src kinase and costimulatory activity enhances signal transduction through single-chain chimeric receptors in T lymphocytes. Blood 2001;98:2364–71.

33. Kowolik CM, Topp MS, Gonzalez S, et al. CD28 costimulation provided through a CD19-specific chimeric antigen receptor enhances *in vivo* persistence and antitumor efficacy of adoptively transferred T cells. Cancer Res 2006;66:10995–1004.

34. Kalikin LM, Schneider A, Thakur MA, et al. *In vivo* visualization of metastatic prostate cancer and quantitation of disease progression in immunocompromised mice. Cancer Biol Ther 2003;2:656–60.